Progress In Electromagnetics Research C, Vol. 61, 91–103, 2016

A 2 × 2 Dual-Band MIMO Antenna with Polarization Diversity for Wireless Applications

Leeladhar Malviya, Rajib K. Panigrahi, and Machavaram V. Kartikeyan*

Abstract—A compact 2×2 dual-band MIMO antenna is proposed with polarization diversity technique for present wireless applications. The proposed design combines the horizontally and vertically polarized radiating elements. The effect of mutual coupling between radiating elements is reduced by partially stepped ground (PSG) and by the orthogonal placement of antenna elements. The whole configuration is designed over a substrate of size $70 \times 70\,\text{mm}^2$. The measured frequency bands extend from 2.408 to 2.776 GHz and 4.96 to 5.64 GHz frequencies with SWR < 2. The measured isolation is more than 21 dB between adjacent and diagonal ports. The measured peak gains at 2.54 GHz, and 5.26 GHz resonant frequencies are 3.98 dBi and 4.13 dBi, respectively. The designed MIMO covers LTE bands (7/38/41), WLAN bands (2.4/5.2 GHz), and WiMAX band (2.5/5.5 GHz). The diversity performances in terms of peak gain, ECC, and MEG have also been reported.

1. INTRODUCTION

In fast growing technology of wireless communication, large bandwidth, high data rate and reliability are the prime objects for indoor and outdoor applications. The multiple radio channels through multiple-input multiple-output (MIMO) technology result in high throughput in non-line-of-sight (NLOS) communications. Due to the compactness of devices, the effect of multiple antennas on the same substrate cannot be ignored. The polarization diversity is one of the techniques able to trans-receive signals in horizontal as well as vertical directions. The following reported works in literature describe various approaches of four-port MIMO antenna designs for high port to port isolation and compactness.

The compactness along with the proper isolation among four radiating elements on the common substrate are very challenging issues and the requirements of present MIMO antennas. The polarization diversity MIMO antenna with dielectric slab was used for the compactness. The overall size of the antenna was $270 \times 210\,\text{mm}^2$, with isolation of 20 dB [1]. Similarly, a spatial and pattern diversity combined technique resulted in a compact size of $90\times60\,\text{mm}^2$, with isolation of 11.5 dB [2]. A broadside and conical polarizations based approach was used with independent feeds and shorting posts to reduce the size of MIMO antenna. The size of the antenna was $200 \times 200\,\text{mm}^2$, with isolation of more than 24 dB [3]. A proximity coupled feed along with the slits (Used as band reject filter) was used for proper impedance match. The isolation level in this case was better than 25 dB. The size of the designed antenna was $60 \times 80\,\text{mm}^2$ [4]. A angular diversity antenna of size $100 \times 120\,\text{mm}^2$ with the multi-beam radiation patterns was designed with reflectors and switches. The combination achieved an isolation of better than 6.7 dB [5].

Similarly, a slotted MIMO antenna with crossed slot and orthogonal polarization diversity was used for isolation improvement. The combination resulted in a compact size of $70.11 \times 70.11\,\text{mm}^2$.

Received 4 November 2015, Accepted 17 December 2015, Scheduled 7 January 2016
* Corresponding author: M. V. Kartikeyan (kartik@iitr.ac.in).
The authors are with the Millimeter/THz Wave Laboratory, Department of Electronics and Communication Engineering, Indian Institute of Technology Roorkee, Roorkee 247667, India.

The measured isolation was better than 24 dB [6]. A cavity backed crossed exponentially tapered slot (CXETS) antenna with polarization diversity (size = $112.3 \times 112.3\,\text{mm}^2$) resulted in an isolation level of more than 25 dB [7]. A crossed feeding network with dual polarizations was used for size reduction and isolation enhancement, also resulted in an omni-directional radiation patterns. The size of the substrate was $200 \times 200\,\text{mm}^2$, and the cross polarization level was better than 20 dB [8]. Similarly, the split ring resonators (SRRs) are one of the choices for size reduction and isolation improvement but at the cost of bandwidth shrinkage. A MIMO antenna was operated in worldwide inter-operability for microwave access (WIMAX) bands using SRRs and parasitic elements. The joint operation of SRRs and parasitic elements resulted in an isolation level of better than 17 dB [9]. The complementary split ring resonator (CSRR) based on four-port MIMO of size $100 \times 50\,\text{mm}^2$, resulted in an isolation level of 10 dB [10]. The effect of the slots on the ground plane is one of the choices for mutual coupling reduction. A common radiating structure of four elements with ground slots was used for wireless fidelity (Wi-Fi)/long term evolution (LTE) applications. The resulting isolation using such slots at the corners was better than 15 dB [11].

Earlier, a 2×1 wide-band MIMO antenna with G shape and protruded ground was designed with 22.5 dB of isolation on substrate of size $55 \times 50\,\text{mm}^2$ [12], and a 1×1 G-shaped monopole with coaxial feed on a substrate of size $40 \times 30\,\text{mm}^2$ was also reported in literature [13].

Most of the described four-port MIMO antennas are big sized or complex structures or having -6 dB impedance bandwidth. In the proposed work, a dual-band MIMO antenna with pattern diversity is presented for high port to port isolation between adjacent and diagonal elements. The proposed MIMO antenna covers LTE bands (7/38/41), WLAN bands (2.4/5.2 GHz), and WiMAX band (2.5/5.5 GHz).

2. DESIGN STUDIES AND RESULTS

The 2×2 MIMO antenna elements with 50 ohm ports are arranged orthogonally to trans-receive signals both in vertical and horizontal directions. The antenna consists of G-shaped elements, PSGs, and one vertical slot in each ground plane. The proposed dual-band MIMO antenna with polarization diversity is designed on an FR4 substrate of size $70 \times 70\,\text{mm}^2$ using computer simulation tool (CST). The FR4 substrate has permittivity of 4.3, loss tangent of 0.025, and thickness of 1.524 mm. The schematic views of radiating element and PSG ground structure for single element are shown in Fig. 1. The design parameters are shown in Table 1. The corresponding 2×2 fabricated MIMO antenna is shown in Fig. 2.

The lower frequency band is due to the effect of the sum of lengths $a + b + c + d + e + f$, where value of $b = 7.10$ mm. The second band is the result of the ground slot and extended arm b. The arm b is extended to reduce the returnloss around 5.0 GHz resonant frequency. The combined effect of ground slot and extended arm b resulted in lower returnloss. The length of the extended arm b is 8.58 mm for the considered design.

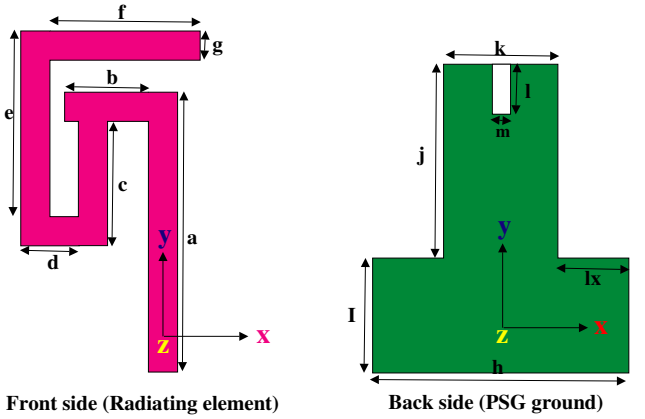

Figure 1. Schematic views of radiating element and PSG ground.

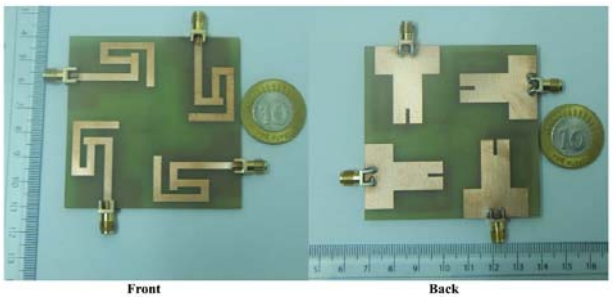

Figure 2. Fabricated 2×2 MIMO antenna.

Table 1. Parameters of the proposed antenna (dimensions in millimeter (mm)).

Parameter	a	b	c	d	e	f	g
Value	28.40	8.58	12.62	5.92	18.93	15.39	2.96
Parameter	h	I	j	k	l	m	lx
Value	26.0	11.66	19.74	11.60	7.43	1.48	7.2

2.1. Simulation and Measurement Results

The proposed MIMO antenna parameters are optimized to get minimum return loss and low mutual coupling using four antenna radiators. For the return loss and isolation measurements using two-port VNA-HP8720B, we connect any of the two ports of the proposed MIMO antenna to the VNA ports through cables, and the remaining ports are terminated by 50 Ω.

The effect of the 1×1 single input single output (SISO) antenna with PSG ground is shown in Fig. 3 on simulated S parameter. A comparison of SISO and the proposed MIMO (2×2) has been carried out to show the effectiveness of the proposed design. It has been observed that without the slot in PSG ground, SISO antenna exhibits 2.348–2.6 GHz and 4.712–4.972 GHZ frequency bands (−10 dB). On the other hand, SISO antenna with the slot in PSG ground shows 2.3456–2.6177 GHz and 4.8726–5.5592 GHz frequency bands. A better response curve is observable here to cover WLAN (2.4/5.2 GHz), and WiMAX (2.5/5.5 GHz) frequency bands. Similarly, when the SISO is converted in 2×2 proposed MIMO antenna, a much better return loss is observable, for both the WLAN bands (2.4/5.2 GHz) and WiMAX bands (2.5/5.5 GHz). A complete description has been shown in the next paragraph for 2×2 proposed MIMO.

It has been observed for 2×2 proposed MIMO that the CST MWS (CST microwave studio version 11) and VNA results are in good agreement. From the simulation and measurement of S parameters, we find that $S_{11} = S_{22} = S_{33} = S_{44}$, $S_{12} = S_{21} = S_{34} = S_{43} = S_{14} = S_{41} = S_{23} = S_{32}$, and $S_{13} = S_{31} = S_{24} = S_{42}$. The symmetry condition exists due to the orthogonal arrangement of antenna elements and PSG planes. Therefore, for the simplicity of analysis, we consider only S_{11}, S_{12}, and S_{13} scattering parameters for the plotting and measurement of other parameters throughout the paper.

The measured and simulated S parameters for return loss and isolation are shown in Fig. 4(a), Fig. 4(b), and Fig. 4(c). Here, we observe that the dual-band antenna has simulated −10 dB impedance bandwidths extend from 2.368 to 2.692 GHz and 4.892 to 5.612 GHz frequencies with SWR < 2. The measured −10 dB impedance bandwidths extend from 2.408 to 2.776 GHz and 4.96 to 5.64 GHz frequencies. The measured isolations between the adjacent and/or diagonal ports in the first and second bands are more than 21 dB. Similarly, the simulated isolation between the adjacent and/or diagonal

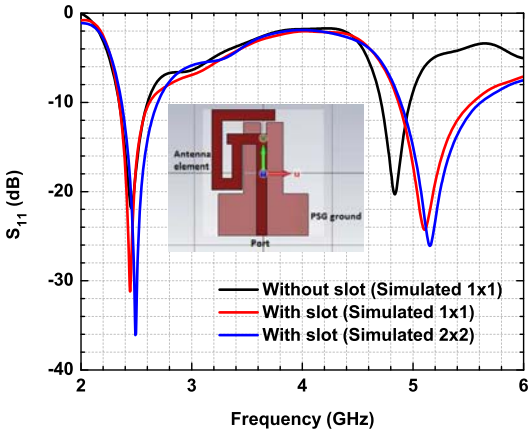

Figure 3. S_{11} parameter of proposed antenna element for SISO (1×1) and MIMO (2×2).

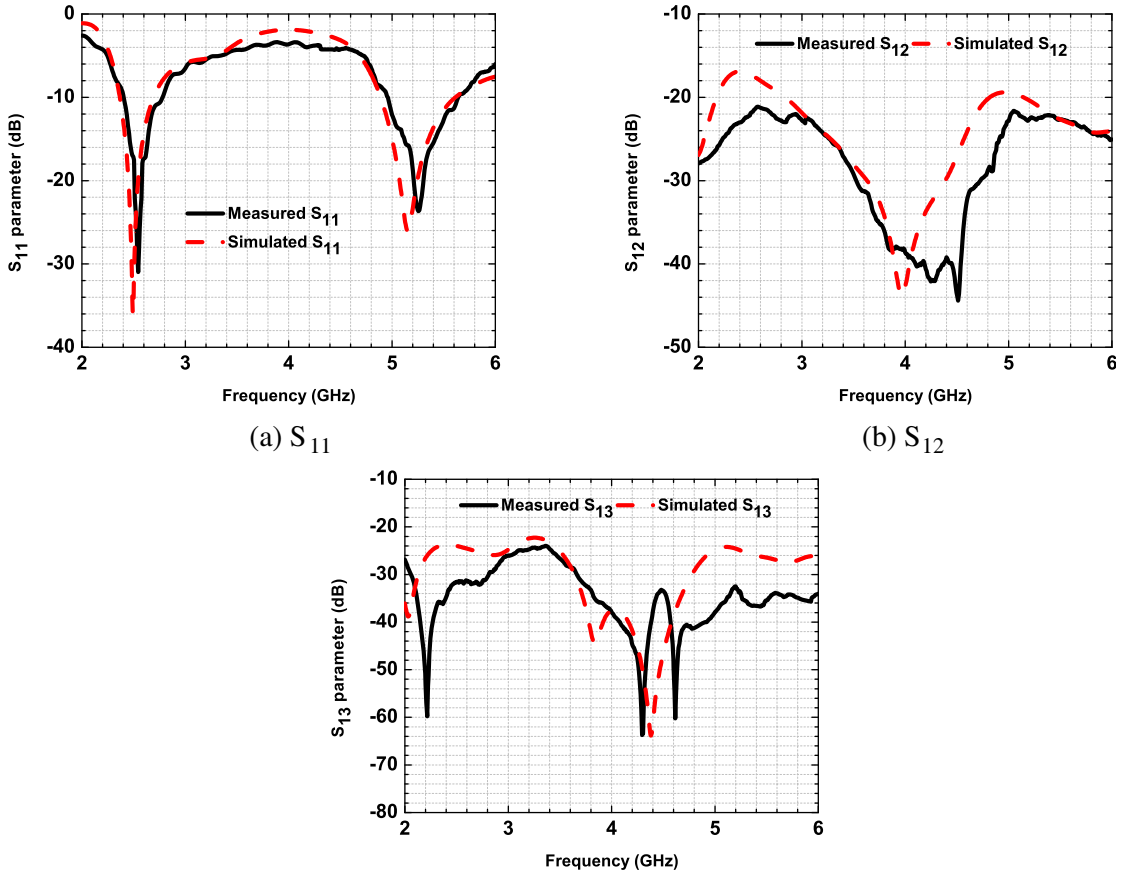

Figure 4. S parameters of proposed 2×2 MIMO antenna.

ports in the first band is more than 17 dB, and in the second band it is more than 19 dB. The various frequency bands are shown in Table 2. The variation in measured and simulated results is due to the fabrication error and port/cable coupling losses.

To see the effect of surface current distribution on the proposed MIMO antenna, any one of the ports is excited, and remaining ports are terminated by 50 Ω. As observable from Fig. 5, high amount of surface current is seen on the left side of the PSG arm and closest arm of antenna element, and a very low amount can be seen on the remaining antenna elements due to current coupling. Its effect can be seen on the lower frequency band on S parameters S_{12} and S_{14}, because antenna elements 2 and 4 are in close proximity with element 1 in comparison to element 3 (In considered design $S_{12} = S_{14}$). Still, due to less current coupling with the terminated elements, isolation is more than 17 dB in lower band. The simulated range of surface current distribution at 2.54 GHz resonant frequency is 0–110 Ampere/metre. Similarly, as observable from Fig. 6, most of the current concentrates on the excited antenna element. Therefore, very low amount of current is coupled to the adjacent and diagonally placed antenna elements. This will result in more than 21 dB of isolation (S_{12} and S_{13}) among all antenna elements in higher frequency band. The simulated range of surface current distribution at 5.26 GHz resonant frequency is 0–44.5 Ampere/metre.

The effect of the extended arm b and ground slot on S parameters can be observed from Fig. 7(a), Fig. 7(b), and Fig. 7(c). It has been observed that the extended arm b along with the ground slot results in lower return loss around the considered frequency band than the other cases (without extended arm b, and without slot). The values of isolations in both the frequency bands show minor fluctuations. The individual effects of arm b and ground slot are also shown in these figures.

Similarly, a comparison between the conventional (full) ground and designed partially stepped

ground (PSG) has been carried out to extend the effects of S parameters on return loss and different isolations. As observable from Fig. 8, the full ground with the MIMO antenna elements results in a single band operation, having a -10 dB returnloss bandwidth of 3.8–3.912 GHz (112 MHZ). It means that bandwidth also gets reduced with the full ground. Another effect of the full ground affects gain value by a very big amount. The value of gain using full ground comes down to 2.7 dB at 3.8 GHz resonant frequency. A very big difference has been observed between S_{12} and S_{13} values while considering these

Table 2. Frequency bands of proposed 2×2 MIMO antenna.

No.	Frequency band	Impedance BW (-10 dB)	Isolation (adjacent and/or diagonal ports)
1	2.408–2.776 GHz (Measured)	0.368 GHz	> 21 dB
2	4.96–5.64 GHz (Measured)	0.680 GHz	> 21 dB
3	2.368–2.692 GHz (Simulated)	0.324 GHz	> 17 dB
4	4.892–5.612 GHz (Simulated)	0.720 GHz	> 19 dB

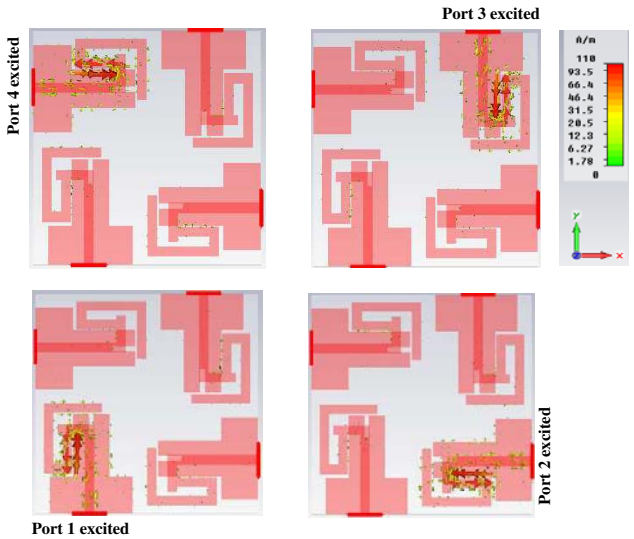

Figure 5. Surface current distribution of proposed 2×2 MIMO antenna at 2.54 GHz.

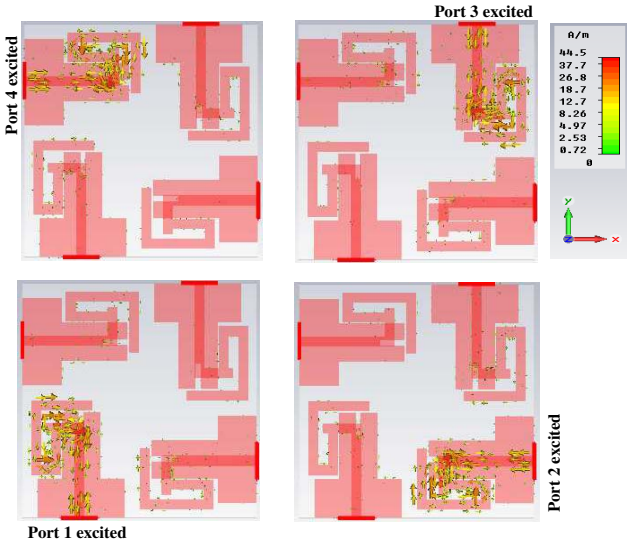

Figure 6. Surface current distribution of proposed 2×2 MIMO antenna at 5.26 GHz.

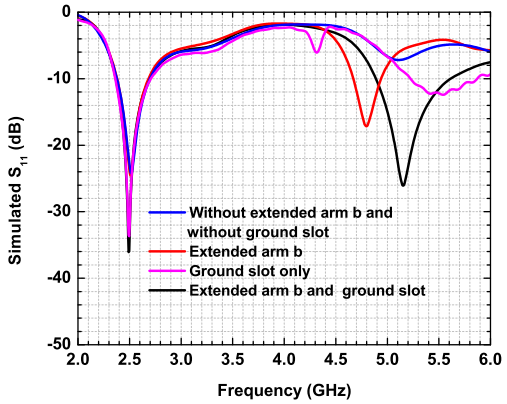

(a) S_{11}

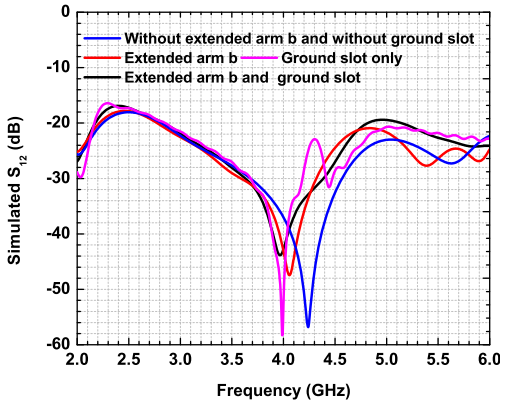

(b) S_{12}

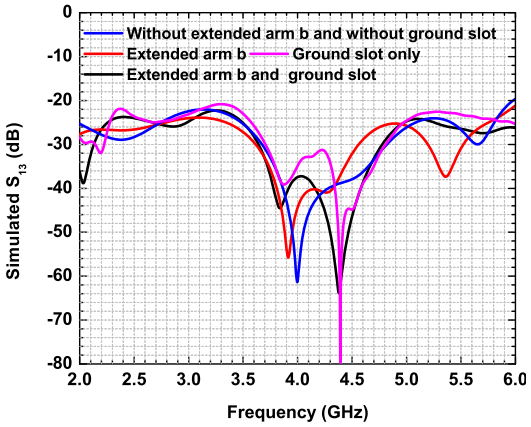

(c) S_{13}

Figure 7. Effects of extended arm b and ground slot on S parameters.

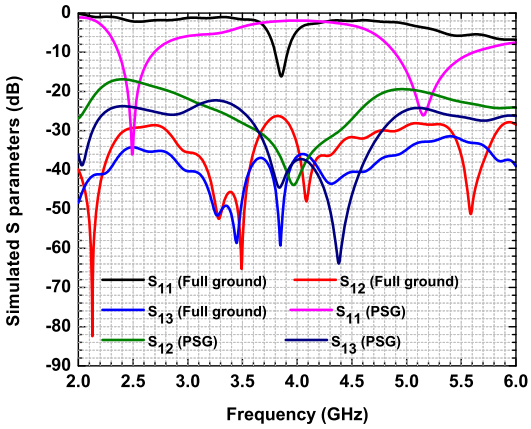

Figure 8. Effects of Full ground and partially stepped ground (PSG) on S parameters.

grounds. The PSG is selected due to the size reduction properties of the ground modification technique and to get the desired resonant conditions. The proposed design is suitable for dual-band and multi-standard operations for various wireless applications, with sufficient isolation between adjacent and diagonal ports.

2.2. Parametric Analysis

The effect of ground slot on S parameters can be observed from Fig. 9(a), Fig. 9(b), and Fig. 9(c). The width of the slot is fixed at 1.48 mm. From the parametric analysis of ground slot length (l) we find that when there is no slot, only two bands are observed around 2.5 GHz and 4.8 GHz frequencies. After the parametric analysis, a slot is etched on ground to get resonance around 5.0 GHz frequency. The length of the slot is selected as 7.43 mm from the top of the central partial ground. We observe that except S_{11}, there are no big changes in isolations S_{12}, and S_{13}.

Similarly, the parametric analysis of arm b on S parameters can be seen from Fig. 10(a), Fig. 10(b), and Fig. 10(c). For the considered design, the length of arm b is selected as 8.58 mm, so that very low return loss can be obtained around 5.0 GHz resonant frequency. It has been observed that for the value of $b = 8.21$ mm, very low return loss is seen in the first band, though a small peak is also seen around 4.35 GHz. It is the main reason that we are considering only $b = 8.58$ mm. We find that S_{11} shows certain variation in different bands with the variation in length of arm b, though there are no big changes in the values of S_{12} and S_{13}.

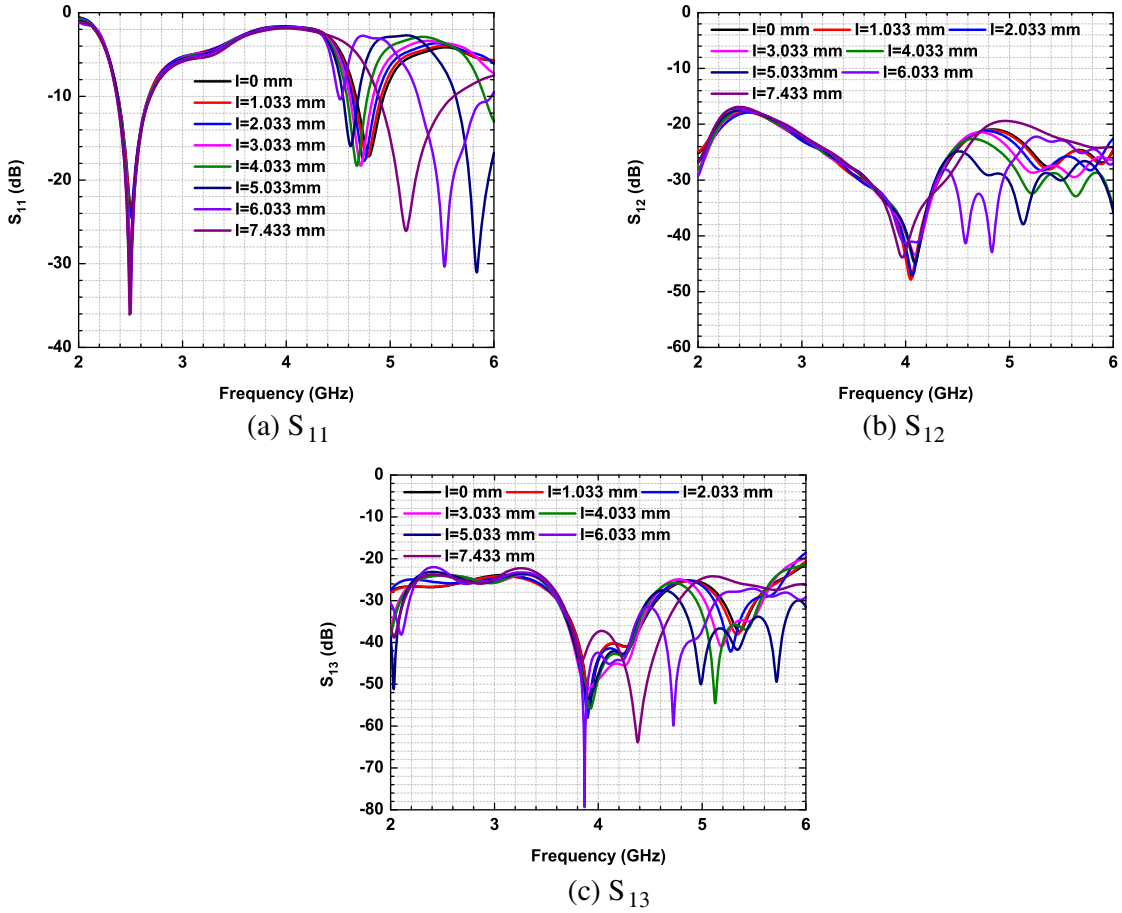

Figure 9. Effect of ground slot length on S parameters.

2.3. Diversity Performance

The diversity performance of the proposed 2×2 polarization diversity MIMO antenna is described in terms of peak gain, efficiency, envelope correlation coefficient (ECC), and mean effective gain (MEG). The measurement of peak gain is performed in an anechoic chamber using the substitution method with two standard horn antennas and the designed antenna. The simulated gains of SISO antenna with slot in PSG ground is more than 2.0 dBi in both the frequency bands. For the proposed MIMO, the simulated peak gains at 2.54 GHz and 5.26 GHz resonant frequencies are 3.948 dBi and 4.022 dBi. Similarly, the measured peak gains at 2.54 GHz, and 5.26 GHz resonant frequencies are 3.98 dBi and 4.13 dBi. The peak gain is a function of the correlation between radiating elements. The measured and simulated results of peak gains have been plotted in Figs. 11(a) and (b).

The efficiency is also one of the diversity parameters. For the proposed polarization diversity MIMO antenna, it is obtained from the CST simulations for lower and higher frequency bands. For the SISO antenna, simulated radiation efficiency is more than 85% in lower band and more than 73.49% in higher band. For the proposed MIMO, as observable from Figs. 11(a) and (b), the radiation efficiencies at 2.54 GHz and 5.26 GHz resonant frequencies are 88.42% and 74.94%. The radiation efficiencies in lower and higher bands are more than 68%. Similarly, the total efficiencies for both the frequency bands are more than 60%.

The next diversity parameter is diversity gain [14], which is obtained in terms of maximum theoretical diversity gain (10 dB) and correlation coefficient using Equation (1). The higher the value of diversity gain is, the better the isolation is and vice versa. The measured values of diversity gains at 2.54 GHz and 5.26 GHz frequencies are 9.94 dB and 9.93 dB. The simulated diversity gains at these resonant frequencies are 10 dB. In both the frequency bands the approximate values of diversity gains

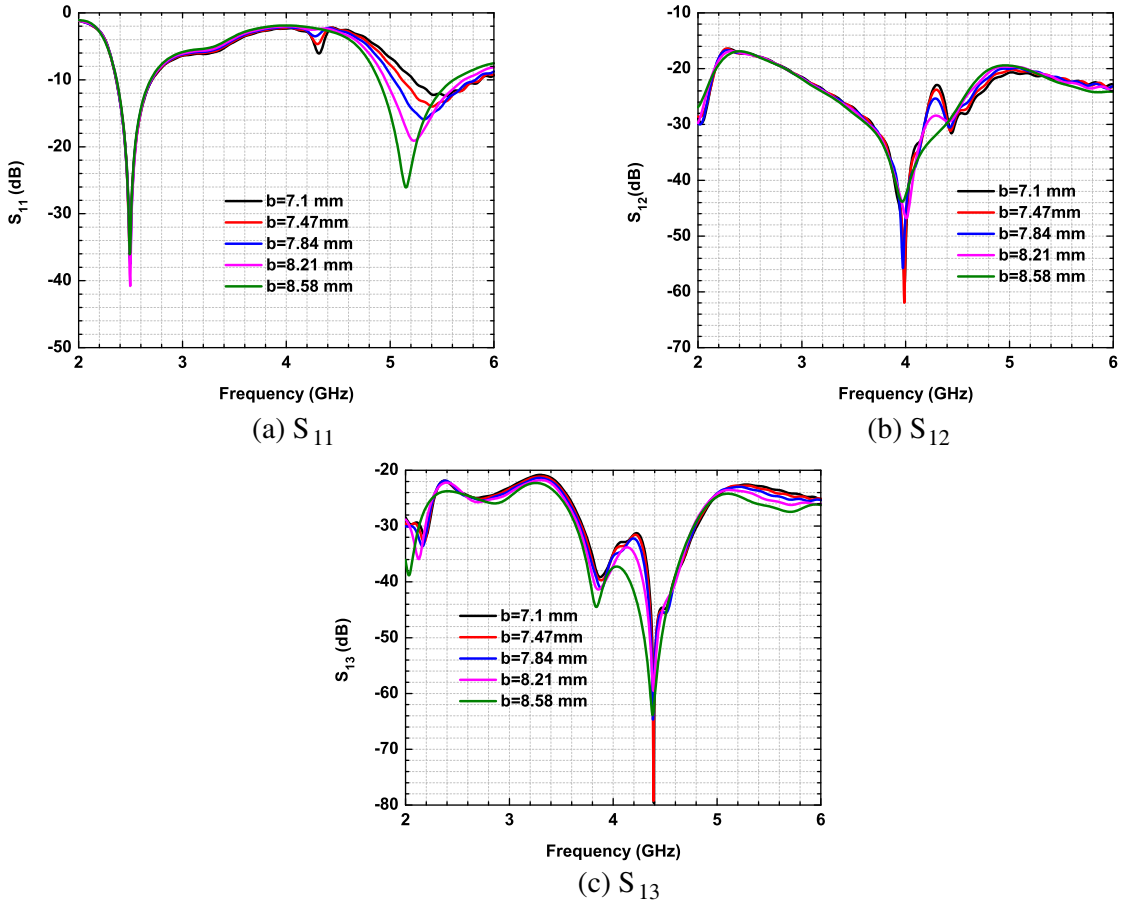

Figure 10. Effect of arm b on S parameters.

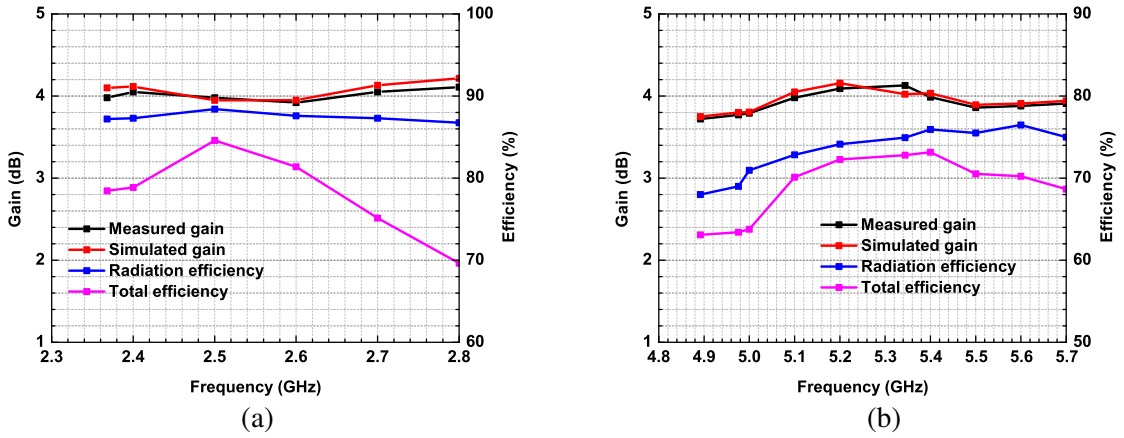

Figure 11. Gain and Efficiencies of proposed 2×2 MIMO antenna. (a) Gain and efficiencies in lower band. (b) Gain and efficiencies in higher band.

are higher than 9.92 dB.

$$G_{DG} = 10 * \sqrt{1 - |\rho|^2} \tag{1}$$

Similarly, the ECC shows a diversity behavior of the proposed MIMO antenna. Lower value of ECC means lower correlation between antenna elements and vice versa. The ECC is so important because it

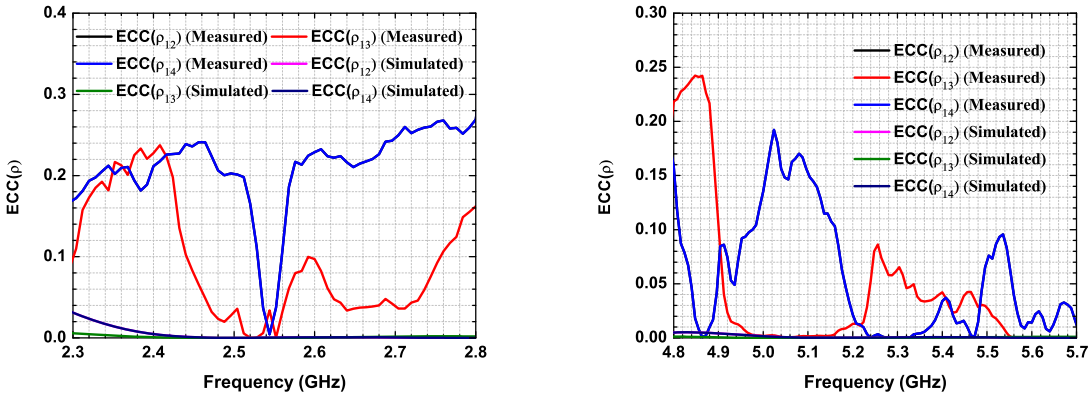

Figure 12. ECC of proposed 2×2 MIMO antenna. (a) ECC in lower band. (b) ECC in higher band.

involves all the S parameters of the designed MIMO antenna. The simulated/measured values of ECC [10] may be obtained using the formula shown in Equation (2). Here the values $i = 1$ to 4, $j = 1$ to 4 for four elements, and $N = 4$ (as total 4 antenna elements).

$$|\rho_e(i,j,N)| = \frac{\left|\sum_{n=1}^{N} S_{i,n}^{*} S_{n,j}\right|}{\sqrt{\left|\prod_{k(=i,j)} \left[1 - \sum_{n=1}^{N} S_{i,n}^{*} S_{n,k}\right]\right|}} \tag{2}$$

The values of ECC for the adjacent and diagonal ports are denoted by ρ_{12}, ρ_{13}, and ρ_{14}, where ρ_{12} is the ECC between antenna elements 1 and 2, similarly ρ_{13} the ECC between antenna elements 1 and 3, and ρ_{14} the ECC between antenna elements 1 and 4. Due to the equi-distance condition between two nearest elements, $\rho_{12} = \rho_{14}$ (both for simulated and measured values). Therefore, only two curves of measured and two curves of simulated results are observable in figures of ECC. As observable from Fig. 12(a) and Fig. 12(b), the simulated values of the ECC between any of the two radiators lies in the range of 0–0.035 in both the frequency bands. Similarly, the measured values of ECC between any of the two radiators lies in the range of 0–0.27 for both the frequency bands. The values of different ECCs for adjacent and diagonal ports are given in Table 3, for both the resonant frequencies. Although the measured results showed very much fluctuation in ECC values, we obtained very low ECCs between any of the two radiators at resonance. The big difference in the measured and simulated ranges/values is due to the fabrication errors and port coupling losses. The value of ECC in both the frequency bands is lower than 0.5, which is also the requirement for 4G applications.

Table 3. ECC of proposed 2×2 polarization diversity MIMO.

Frequency (GHz)	ECC (Simulated)			ECC (Measured)		
	ρ_{12}	ρ_{13}	ρ_{14}	ρ_{12}	ρ_{13}	ρ_{14}
2.54	2.54×10^{-4}	7.54×10^{-6}	2.54×10^{-4}	0.00434	0.034	0.00434
5.26	4.24×10^{-4}	3.72×10^{-6}	4.24×10^{-4}	0.00167	0.074	0.00167

The MEG is also the diversity parameter and is measured in an anechoic chamber for the far field. The MEG [10] includes efficiency and power patterns of the proposed MIMO antenna. Let the cross-polarization ratio of the incident field denoted by XPR. The probability distribution functions (pdf) of the incident wave are $p_{\theta j}$ and $p_{\phi j}$ for θ and ϕ components. The power gains of the proposed 2×2

MIMO antenna elements are $G_{\theta j}$ and $G_{\phi j}$. The value of j is 1 to 4 for four elements. The formula of MEG is given in Equation (3).

$$MEG_j = \oint \left(\frac{XPR}{1+XPR} P_{\theta j}(\Omega) G_{\theta j}(\Omega) \; + \frac{1}{1+XPR} P_{\phi j}(\Omega) G_{\phi j}(\Omega) \right) \tag{3}$$

The above equation of MEG can also be written as shown in Equation (4).

$$MEG_j = \frac{1}{2\pi} \int_0^{2\pi} \left[\frac{XPR}{1+XPR} G_{\theta j}\left(\frac{\pi}{2}, \phi\right) + \frac{1}{1+XPR} G_{\phi j}\left(\frac{\pi}{2}, \phi\right) \right] d\phi \tag{4}$$

Let us consider that the horizontal and vertical components of the gaussian signals have mean $(\mu) = 0$ and variance $(\sigma) = 20$, respectively. A comparison between the isotropic medium and Gaussian medium has been carried out in Fig. 13, for different values of XPR and MEGs using CST simulation. It has been observed that due to the indoor and outdoor environments, changes are observable for XPR = 0 dB and XPR = 6 dB. This is due to the variation in received power in that direction for the values of θ and ϕ. The different values of MEGs for isotropic and gaussian mediums are obtained using CST simulations and are shown in Table 4 (due to symmetry of radiating structure value is common for each radiating element). For practical cases, different values of MEGs may be obtained for different antenna elements. However, in the case of CST simulations only constant value of MEG is shown for MIMO for that frequency. Therefore, from the observations, it is seen that the antenna provides good diversity performance in terms of MEG.

Table 4. CST simulated MEGs at different frequencies for proposed design (dB).

Frequency (GHz)	Isotropic medium		Gaussian medium	
	MEG (XPR = 0 dB)	MEG (XPR = 6 dB)	MEG (XPR = 0 dB)	MEG (XPR = 6 dB)
2.54	−4.68	−6.6	−5.3	−8.5
5.26	−5.758	−6.0	−7.9	−9.1

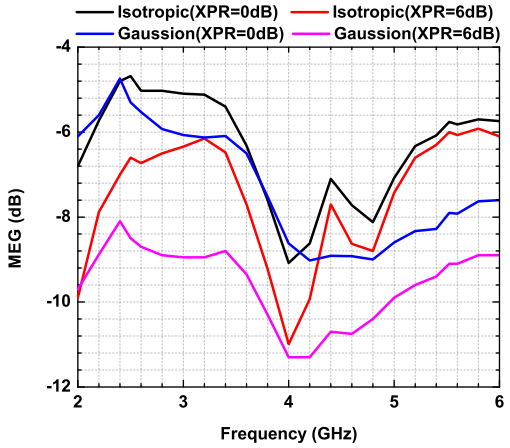

Figure 13. MEG comparisons between isotropic and gaussian mediums.

2.4. Far Field Radiation Patterns

The measurement is carried out in an anechoic chamber in the presence of a standard horn antenna, which is used as a transmitting antenna. During the measurement, when any one radiator is used in receiving mode, the other ports are terminated by 50 Ω to avoid any signal pick up. The far-field radiation patterns of 4-port polarization diversity MIMO antenna are measured at 2.54 GHz and 5.26 GHz resonant frequencies.

The simulated E- and H-plane field patterns for SISO antenna are shown in Fig. 14. These are the results to show the effectiveness of the considered antenna element and the corresponding PSG ground. For the 2×2 MIMO, the effect of simulated far field on the E- and H planes can be described using E_θ, E_ϕ, H_θ, and H_ϕ components. The effect of E- and H-fields on both the components (θ and ϕ) can easily be seen. As observable from Fig. 15 and Fig. 16, these components also verify the implementation of polarization diversity between two field components.

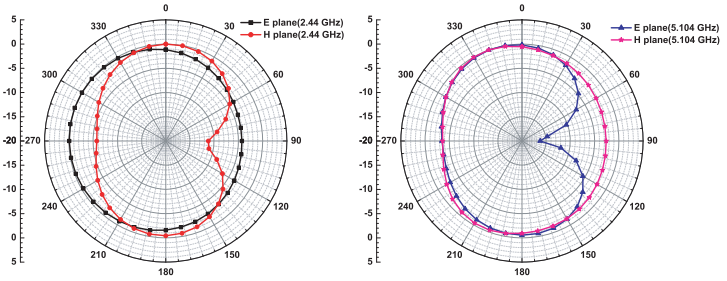

(a) 2.44 GHz (b) 5.104 GHz

Figure 14. Simulated E field and H field radiation patterns of SISO (x-y plane).

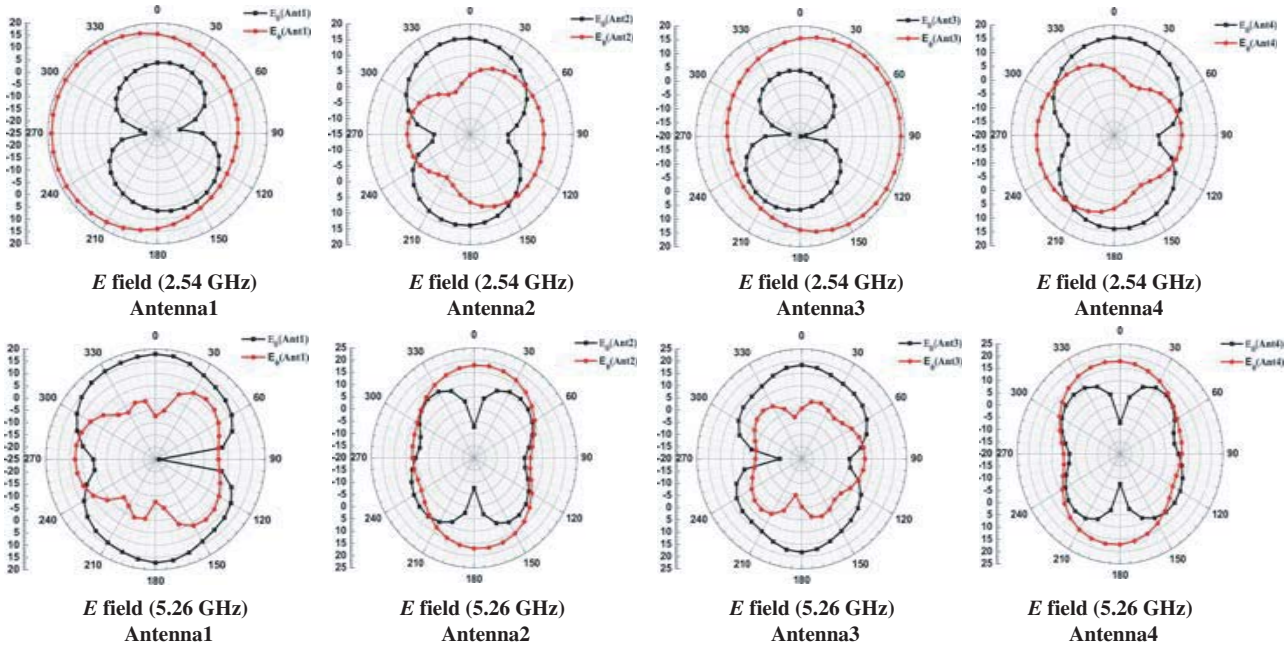

Figure 15. Simulated E_θ and E_ϕ radiation patterns of proposed MIMO (Ant: Antenna element).

The measured and CST simulated E plane (absolute) and H plane (absolute) field patterns of the proposed MIMO antenna are compared in Fig. 17 and Fig. 18 for x-y plane. The MIMO antenna elements 1 and 3, and 2 and 4 are complementary symmetric for each resonant case. This is due to the placement of one component in horizontal and other component in vertical position. Due to this, antenna elements 1 and 3, and 2 and 4 show complementary symmetry. We observe certain discrepancies between simulated and measured patterns due to the errors in fabrication process and port/cable coupling losses. Also the unequal scale can be seen even after the normalization of the E plane (absolute) and H plane (absolute) field patterns. This is possibly due to the θ and ϕ component values in simulated and measured results.

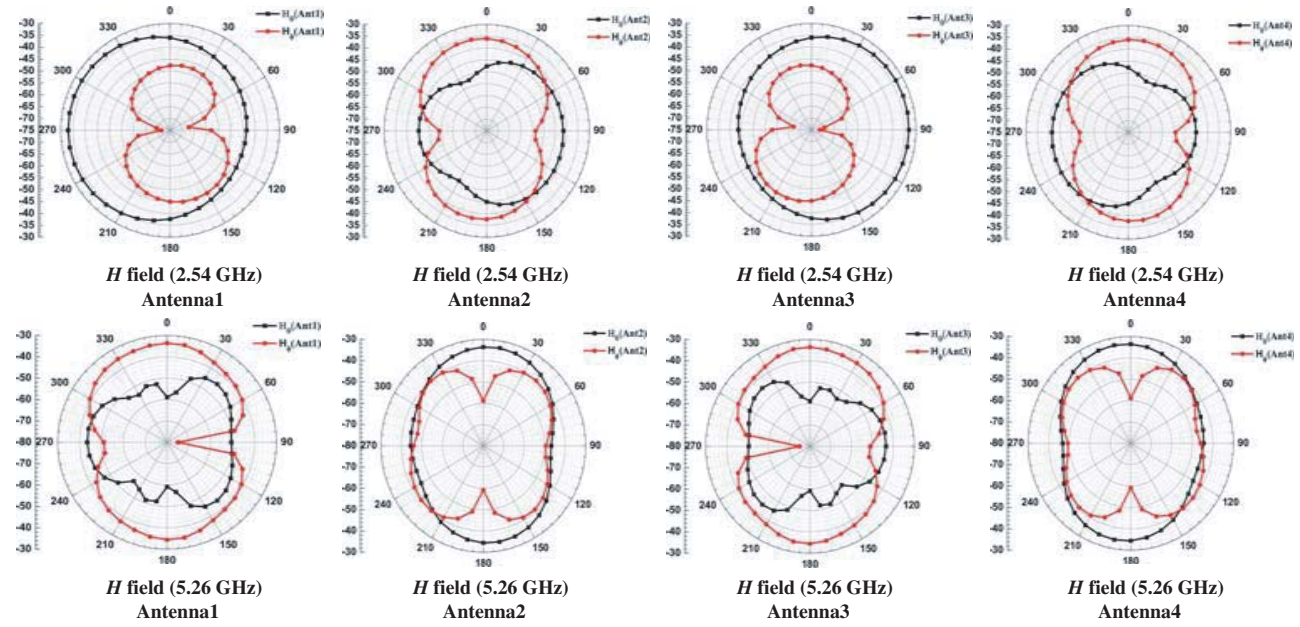

Figure 16. Simulated H_θ and H_ϕ radiation patterns of proposed MIMO (Ant: Antenna element).

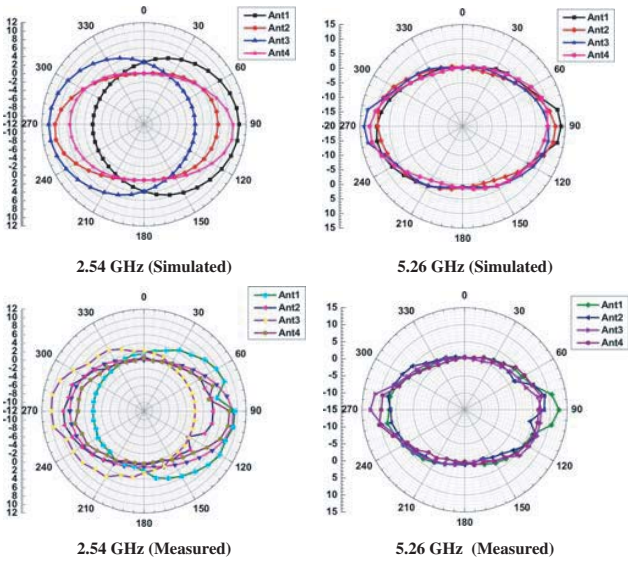

Figure 17. E field radiation patterns of proposed MIMO antenna (x-y plane) (Ant: Antenna element).

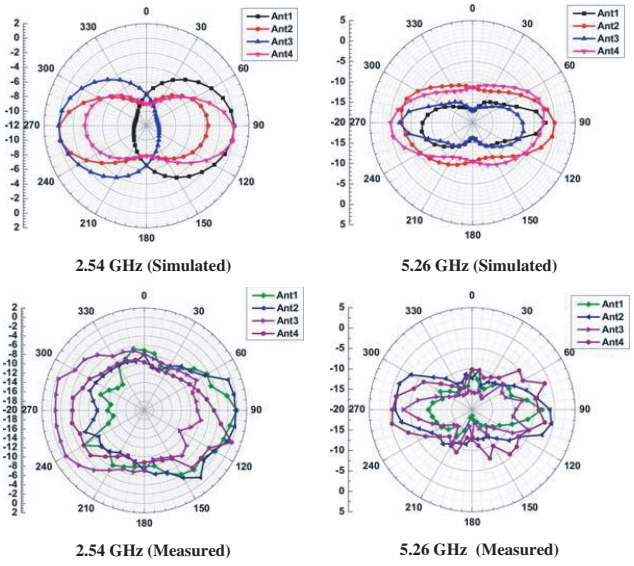

Figure 18. H field radiation patterns of proposed MIMO antenna (x-y plane) (Ant: Antenna element).

3. CONCLUSIONS

A compact four-element dual-band MIMO antenna is proposed with polarization diversity technique for present wireless communication. The proposed MIMO antenna is a combination of orthogonally arranged antennas. The effect of mutual coupling between radiating elements is reduced by the orthogonally arranged ground for each antenna. The measured frequency bands cover the 2.408–2.776 GHz and 4.96–5.64 GHz frequency bands. The measured isolation in each frequency band is more than 21 dB between radiating elements. The measured gains at 2.54 GHz and 5.26 GHz resonant

frequencies are 3.98 dBi and 4.13 dBi, respectively. The proposed design covers LTE bands (7/38/41), WLAN bands (2.4/5.2 GHz), and WiMAX band (2.5/5.5 GHz). The measured ECC is very low at resonant frequencies.

REFERENCES

1. Yeap, S. B., X. Chen, J. A. Dupuy, C. C. Chiau, and C. G. Parini, "Integrated diversity antenna for laptop and PDA terminal in a MIMO system," *IEE Proceedings Microwave Antennas Propagation*, Vol. 152, No. 6, 495–504, 2005.
2. Ding, Y., Z. Du, K. Gong, and Z. Feng, "A four element antenna system for mobile phones," *IEEE Antennas and Wireless Propagation Letters*, Vol. 6, 655–658, 2007.
3. Yang, S. L. S., K. M. Luk, H. Lai, A. A. Kishk, and K. F. Lee, "A dual polarized antenna with pattern diversity," *IEEE Antennas and Propagation Magazine*, Vol. 50, No. 6, 71–79, 2008.
4. Li, H., J. Xiong, and S. He, "A compact planar MIMO antenna system of four elements with similar radiation characteristics and isolation structure," *IEEE Antennas and Wireless Propagation Letters*, Vol. 8, 1107–1110, 2009.
5. Chang, D. C., B. H. Zeng, and J. C. Liu, "Reconfigurable angular diversity antenna with quad corner reflector arrays for 2.4 GHz applications," *IET Microwaves Antennas and Propagation*, Vol. 3, No. 37, 522–528, 2009.
6. Zhang, S., P. Zetterberg, and S. He, "Printed MIMO antenna system of four closely spaced elements with large bandwidth and isolation," *Electronics Letters*, Vol. 46, No. 15, 1052–1053, 2010.
7. Costa, J. R., E. B. Lima, C. R. Medeiros, and C. A. Fernandes, "Evaluation of a new wideband slot array for MIMO performance enhancement in indoor WLANs," *IEEE Transactions on Antennas and Propagation*, Vol. 59, No. 84, 1200–1206, 2011.
8. Sim, C. Y. D., "Conical beam array antenna with polarization diversity," *IEEE Transactions on Antennas and Propagation*, Vol. 60, No. 10, 4568–4572, 2012.
9. Ntaikos, D. K. and T. V. Yioultsis, "Compact split ring resonator loaded multiple input multiple output antenna with electrically small elements and reduced mutual coupling," *IET Microwave Antennas and Propagation*, Vol. 7, No. 6, 421–429, 2013.
10. Sharawi, M. S., M. U. Khan, A. B. Numan, and D. N. Aloi, "A CSRR loaded MIMO antenna system for ISM band operation," *IEEE Transactions on Antennas and Propagation*, Vol. 61, No. 8, 4265–4274, 2013.
11. Moradikorordalivand, A., T. A. Rahman, and M. Khalily, "Common elements wideband MIMO antenna system for WiFi/LTE access point applications," *IEEE Antennas and Wireless Propagation Letters*, Vol. 13, 1601–1604, 2014.
12. Xia, X.-X., Q.-X. Chu, and J.-F. Li, "Design of a compact wideband MIMO antenna for mobile terminals," *Progress In Electromagnetics Research C*, Vol. 41, 163–174, 2013.
13. Sankar, K., R. Bargavi, Samson, and S. Arivumani, "Single layer dual-band G-shaped patch antenna," *International Conference on Communication and Signal Processing*, 636–639, India, April 2014.
14. Singh, H. S., G. K. Pandey, P. K. Bharti, and M. K. Meshram, "A compact dual-band diversity antenna for WLAN applications with high isolation," *Microwave and Optical Technology Letters*, Vol. 57, No. 4, 906–912, 2015.